

Aplestia: The effect of high levels of foreign gene expression on the electrical properties of *Neurospora crassa*¹.

Rachel Giblon² and Roger R. Lew, Biology Department, York University

Revision 1.1 (25 April 2013)

OBJECTIVE

To determine whether high levels of GFP-tagged histone in nuclei affect the ion transport properties of *Neurospora crassa*.

¹ Copyright 2013

² Biophysics Research Assistant. Experiments were performed 01SEP2013 through 31APR2013 in the Lew Laboratory (RRL email: planters@yorku.ca) and were funded in part by NSERC (Natural Sciences and Engineering Research Council)

INTRODUCTION

Green fluorescent protein is extraordinarily important for researchers. Shimomura, Chalfie and Tsien won the Nobel Prize for its discovery (Nobel, 2008). Because it is possible to create fusion proteins that incorporate green fluorescent protein, it is possible to follow the fate of the proteins using fluorescence microscopy. Thus, the expression of proteins can be followed dynamically, and protein activity can be monitored (Tsien, 1998). In our lab, Aryan Abadeh is tracking the movement of nuclei in a *Neurospora crassa* strain that expresses histone tagged with green fluorescent protein. Although this is a common way to use green fluorescent proteins, we don't know whether the expression of high levels of the tagged histone in the nuclei has a deleterious effect on gene expression in general, and as a result, on the physiological health of the fungus. Therefore, I measured the electrical properties of the GFP-expressing strain and compared it to wildtype. Ion transport not only causes the electrical properties of the fungus, but also is vital for its growth. Thus, it is a useful metric for monitoring the physiological status of the fungus.

Measuring the electrical properties. Concentration gradients are a fundamental part of cell life, since a myriad of cellular activities are maintained and controlled by changes in solute flux. The Nernst equation (outlined below) relates the numerical value of the *ion* concentration gradient to the electric potential that balances it.

$$E_N = \frac{RT}{zF} \ln \left(\frac{P_N [c_o]}{P_N [c_i]} \right) \quad (\text{eqn 1.0})$$

Here E_N is the Nernst potential, R the gas constant, T the temperature in Kelvins, z the ion charge, F the Faraday constant, c_o the concentration of the ion outside and c_i the concentration of the ion inside. For a monovalent ion, RT/F is equal to about 25 mV at room temperature (295 K).

The Nernst equation *only* works for a single ion species diffusing across a membrane. For biological membranes, there are *multiple* ions. So, we must use the Goldman-Hodgkin Katz equation, which includes terms for each ionic species of interest, and their respective permeabilities.

$$E_G = \frac{RT}{F} \ln \left(\frac{P_K [c_K^{outside}] + P_{Na} [c_{Na}^{outside}] + P_H [c_H^{outside}] + P_{Cl} [c_{Cl}^{inside}]}{P_K [c_K^{inside}] + P_{Na} [c_{Na}^{inside}] + P_H [c_H^{inside}] + P_{Cl} [c_{Cl}^{outside}]} \right) \quad (\text{eqn 1.1})$$

In cells, we also need to consider active transport of solutes across the membrane against their concentration gradient. Accounting for both active and passive ion transport, we can summarize our expression for total electrical potential across the membrane as:

$$E_M = \frac{I_{pump}}{g_m} + E_G \quad (\text{eqn 1.2})$$

That is, the membrane potential is the sum of total pump current (I_{pump}) divided by the conductance (g_m) and the Goldman-Hodgkin Katz potential for permeant ions (E_G).

For the fungus *Neurospora crassa* (and the yeast *Saccharomyces cerevisiae*), the major source of ionic pump current across the plasma membrane is a H⁺-ATPase pump (Serrano, 1984). Often called the “proton pump”, the H⁺-ATPase pump utilizes the cell’s ATP energy stores to pump H⁺ out of the cell. The net positive charge efflux creates a negative inside electrical potential (I_{pump} / g_m). In order to assess the contribution of active transport to the cell’s electrogenicity, we treated the fungal hyphae with cyanide to deplete cellular ATP and therefore inhibit H⁺-ATPase activity. Cyanide is highly toxic to most organisms, fatal at a high enough dosage. Remarkably, *Neurospora* possess an alternate oxidase pathway, in conjunction with cyanide degrading enzymes that enable cyanide resistance (Deschaneau *et al.*, 2005). It takes some time to activate the alternate oxidase pathway, so it is possible to measure the passive diffusion contribution to electrogenicity (E_G) immediately after cyanide inhibition (which causes a depolarization of the membrane potential). To observe the electrical properties of both active ion pumps and passive ionic diffusion, I measured the current-voltage relationship before and after treatment with cyanide solution.

MATERIALS AND METHODS

Strains. Stock cultures of wild-type *N. crassa* (strain 74-OR23-1VA, FGSC 2489) and his-tagged GFP (strain rid Pccg-1-hH1⁺-sgfp⁺, FGSC 10174) were grown and maintained on Vogel's minimal medium plus 1.5% (w/v) sucrose and 2.0% (w/v) agar (VM) (Vogel, 1956). The major ions in VM (in mM) are: K⁺ (36.7), P_i (36.7), Na⁺ (25.5), NH₄⁺ (25), NO₃⁻ (25), citrate (8.5), Cl⁻ (1.36), Mg²⁺ (0.81), SO₄²⁻ (0.81), and Ca²⁺ (0.68); pH is 5.8 (Lew, 2007).

Culture preparation for experiments. Conidia from stock cultures were placed in Petri dishes on cellophane dialysis tubing (2.5 x 6 cm) (molecular weight cutoff, 12,000 to 14,000) overlaying a VM agar plate. Transfer of the conidia was done along one side of the plate, so that the colony would grow across the plate from one side to the other. Cultures were grown overnight (in the dark) at 28°C. Cellophane sections of approximate size 1x3 cm containing the growing edge of the colony were cut and transferred to the inside cover of a 30 mm Petri dish and attached to the center of the dish using masking tape. Then, 3–4 ml of buffer solution (BS) was added to the plate to submerge the colony. BS contains (in millimolar concentrations): KCl (10), CaCl₂ (1), MgCl₂ (1), sucrose (133), and the buffer morpholineethanesulfonic acid (MES) (10); pH was adjusted to 5.8 using 5 N KOH. The colony edge was then observed to ensure that hyphal tip growth had recommenced before electrical measurements were taken. For impalements, I selected large trunk hyphae (10–20 μm diameter) *in situ*, with visible cytoplasmic flow about 0.5 cm behind the colony edge. Wild type and his-tagged GFP strain measurements were typically interspersed during experimental runs.

Electrical Measurements. Hyphae were impaled using two single barrel micropipettes (Hamam and Lew, 2012) made from borosilicate glass capillaries (1.0 mm OD, 0.58 mm ID with an internal filament; Friedrich and Dimmock Inc., Millville, NJ). The capillaries were pulled to a fine point with a model P-30 micropipette puller (Sutter Instrument Co., Novato, CA). Micropipettes were filled with 3 M KCl solution and placed into microelectrode holders containing an Ag/AgCl electrode. The microelectrodes were connected to IE-251A electrometers (input impedance, 10¹¹ Ω; Warner Instruments). Typically, microelectrodes had tip resistances of about 5 MΩ. The circuit was completed with a salt bridge containing 3 M KCl in 2% (w/v) agar and an Ag/AgCl electrode. The two impalements were performed about 10 to 20 μm apart (Figure 1). Following the second impalement, a voltage clamp measurement was performed using an operational amplifier configured for voltage clamp that was controlled by a data acquisition board (Scientific Solutions, Solon, OH). The clamping protocol was a bipolar stepwise staircase of alternating positive and negative voltage clamps and resting potential with a clamping duration of 200 ms (the clamp duration guaranteed that clamping currents were at steady state). Samples of both the clamping current and the clamped voltage were taken during the last 10 ms. For current-voltage measurements, three replicate measurements were performed before and after cyanide treatment, and averaged. Variability was quite low for the three replicates (Figure 2). For comparisons between wildtype and the his-tagged GFP strain, 18 experiments were performed, for the most part interspersing measurements of each strain.

Cable properties of the hyphae must be considered when quantifying the current density (mA/m²). Attenuation of the voltage change at sites distal sites to the site of impalement is exponential, described by the equation $V_x/V_0 = e^{(-x/\lambda)}$, where V_x is the voltage at distance x , V_0 is

the voltage at the current injection site, x is the distance, and λ is the length constant. Using a cylindrical geometry as an approximation for the hyphae, the current density (I_m) can be calculated as $I/(2\pi d\lambda)$, where I is the clamping current, d is the diameter of the impaled hypha, and λ is the length constant of the hyphae. Previous measurements of voltage attenuation along hyphae under preparation and measurement conditions identical to those in the experiments (Lew, 2007) provided a length constant of 407 μm . Occasionally, clamping currents at the extreme negative and positive voltages were clipped, compromising the fidelity of the voltage clamp. Any clipped clamping currents were not included in conductance calculations (mS/m^2) (estimated from the slopes of linear regression fits of the current-voltage relations).

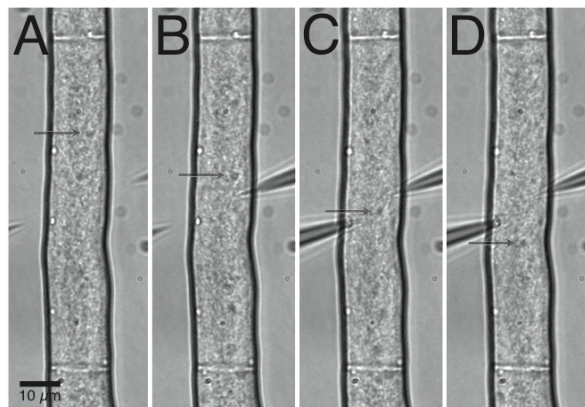


Fig. 1. Method of hyphal impalement and equivalent circuit representation.

(Upper panel) Dual impalement of a hyphal segment (A) Selected hyphae prior to impalement (B) First impalement. (C) Second impalement. (D) After second impalement. Bar, 10 μm .

(Lower panel) The equivalent electrical circuit of the hyphal segment. The hypha is modelled as a cylinder, with the cell membrane resistances in series along its length. Current passes outward through the membrane into a grounded external medium. The clamping current is attenuated exponentially with increasing distance from the site of impalement. Corrections for the cable properties of the hypha are described in Materials and Methods.

Image taken from Hamam and Lew (2012).

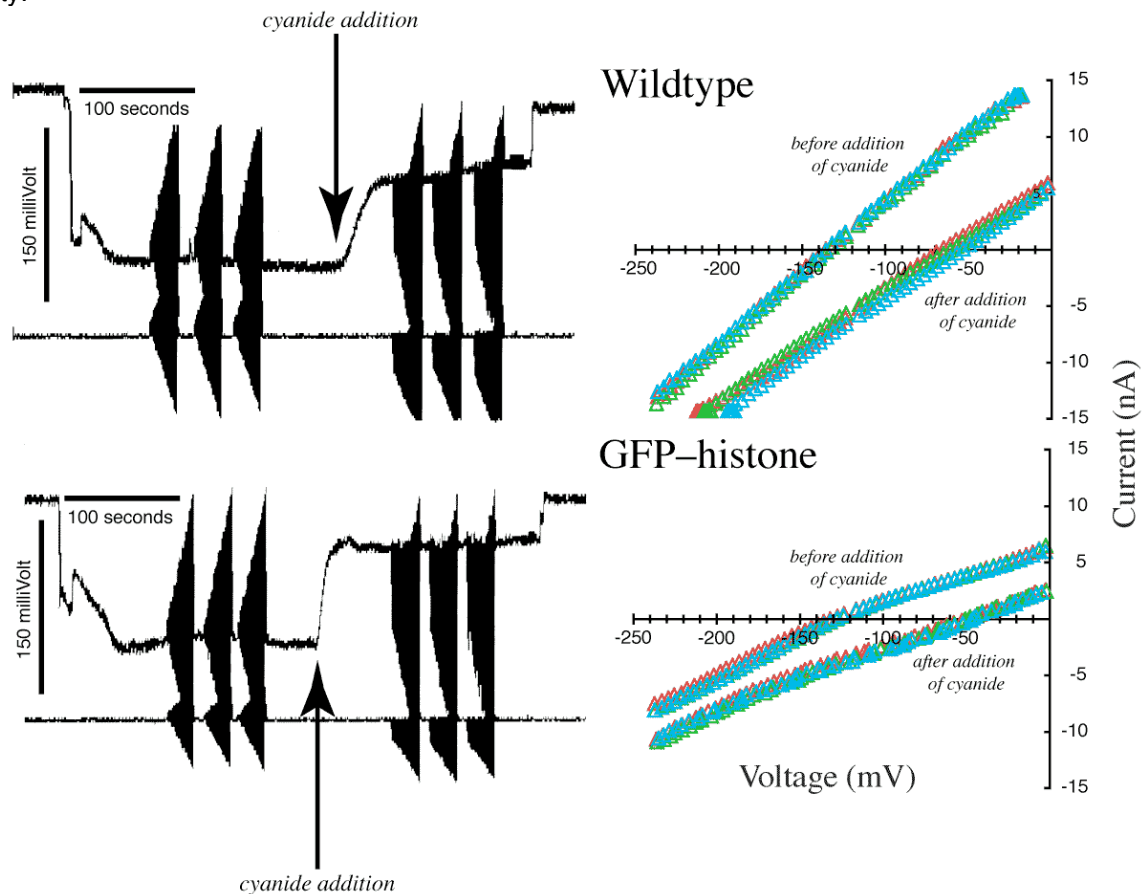
When measuring current densities, one significant area of concern is the effect of multiple impalements on membrane resistance. Often, the performance of a dual impalement is accompanied by a variable — but usually slight — decrease in the measured potential. That is, the impalements may cause an alternate path of low resistance (shunt resistance) across the membrane at the sites of impalement. This attenuates the measured voltage across the membrane

because of voltage dividing. This result can be seen as a depolarized potential after the second impalement compared to the initial potential after the first impalement (Figure 3). As well, the effect of the impalements will differ depending on the care taken during the impalement and the extent of the recovery by the impaled hyphae. Overall, the change is fairly small, so no attempt was made to correct for shunt resistance. However, it does lead to higher clamping currents and consequently to an overestimate of current density by approximately 10%.

RESULTS

Electrical properties of his-tagged GFP mutants and wild type strains. In order to find out the respective roles of passive ion diffusion (Goldman-Hodgkin Katz potential) and active transport (H^+ -ATPase pump), three measurements of current-voltage relations were performed prior to incubation with cyanide. After cyanide addition, when the depolarization of the potential was near steady state, another three current-voltage measurements were taken. A ‘representative’ example of the electrical measurements in the two strains and the current-voltage relations are shown in Figure 2. These experiments were replicated 18 times for each of the strains. The

Fig. 2. Electrical trace of membrane potential and current-voltage relation before and after cyanide treatment. (Left) Electrical traces of voltage change over time. Peaks at the onset of depolarization indicate second impalement. Ionic pump inhibition can be seen in membrane depolarization following cyanide addition. Traces of three current-voltage relation measurements are shown for both before and after cyanide. (Right) Current-voltage relations before and after cyanide treatment. Measurements of the his-tagged GFP strains (bottom) were interspersed with measurements of the wild type (top) as a control. The three measurements taken both before and after cyanide treatment are shown in the red, blue and green triangles. The data have been corrected for the cable properties of the hyphae, as described in Materials and Methods. Standard deviations are not shown, for the sake of clarity.



average current-voltage relations for each strain are shown in Figure 3. Resting potential and conductance measurements are compiled in Figures 4 and 5, respectively.

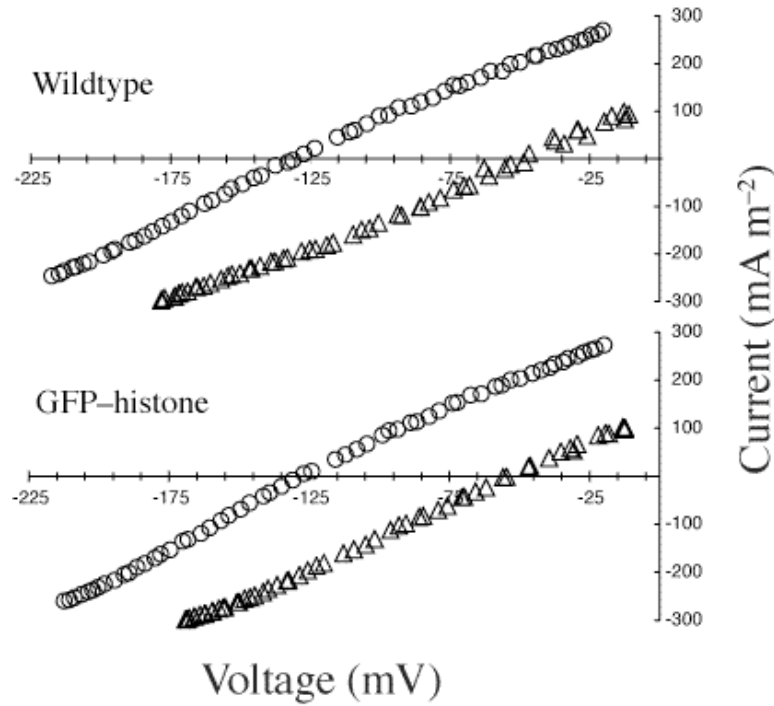


Fig. 3. Average current-voltage relations before and after cyanide treatment.

Measurements of the wildtype (upper panel) and his-tagged GFP strain (lower panel). Circles, before cyanide; triangles, after cyanide. Only mean values are shown ($n = 18$ experiments); standard deviations are not (for the sake of clarity).

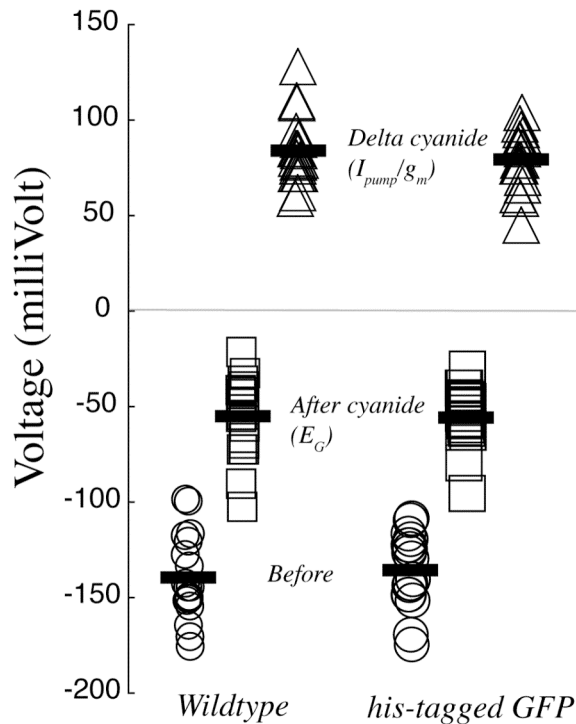
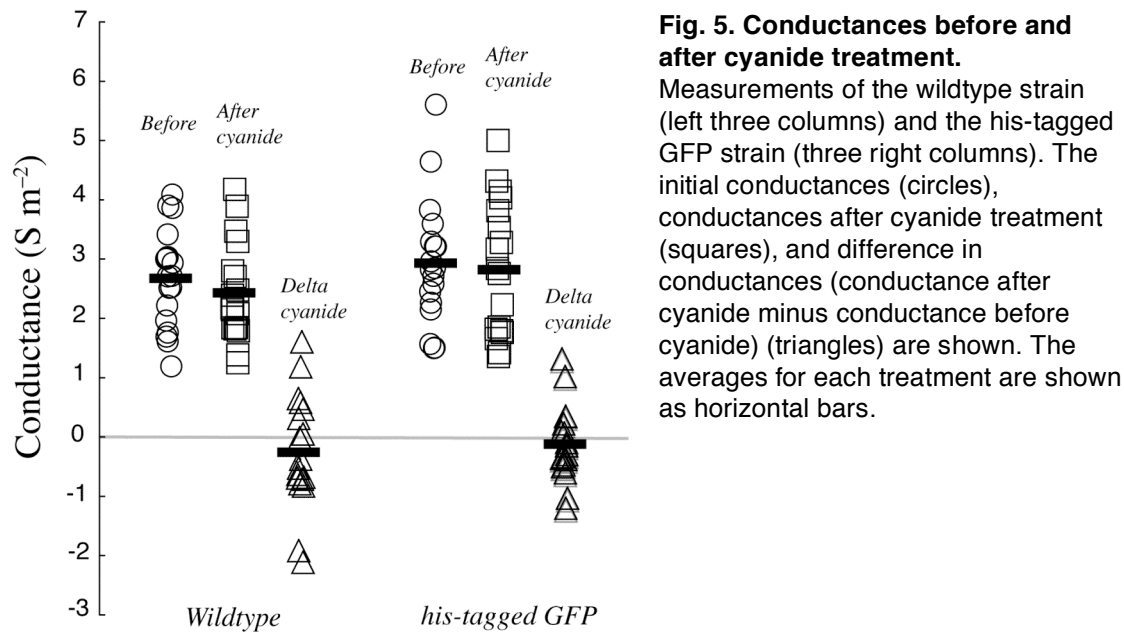


Fig. 4. Resting potentials before and after cyanide treatment. Measurements of the wildtype strain (left three columns) and the his-tagged GFP strain (three right columns). The initial potentials (circles), potentials after cyanide treatment (squares), and difference in potential (potential after cyanide minus potential before cyanide) (triangles) are shown. The averages for each treatment are shown as horizontal bars.



The current-voltage relations of wildtype and the his-tagged GFP strain and wild type were very similar. Slight differences observed in the representative traces (Figure 1) can be attributed to biological variation between hyphae (and colonies used for the experiments). This is confirmed by the results in Figure 2, which show nearly identical average current-voltage relations between the two strains.

The average resting potentials for his-tagged GFP mutants do not vary from those found in wild type strains, both before and after cyanide treatment. T-test values were performed for all permutations and the slight differences were not statistically significant.

The conductances of the wildtype and his-tagged GFP strains were also very similar both before and after cyanide treatment. Wild-type colonies showed a larger spread of conductance change after incubation with cyanide, and a greater average decrease in conductance. None of the slight differences were statistically significant.

DISCUSSION

The utilization of his-tagged GFP mutants has proven to be an invaluable asset in investigating the dynamic features of *Neurospora crassa*. This is true not only in our own laboratory, where they are currently being used to track the movement of nuclei, but for other researchers studying the molecular structure and development of *Neurospora* (Freitag *et al.* 2004, Patterson *et al.* 1997). Does gene over-expression affect the physiological function of *Neurospora*? There is no noticeable difference in the growth rates of the his-tagged GFP compared to wildtype, but more subtle effects might exist. After all, histones play an important role in the packaging of DNA in the nuclei, and the GFP tag could affect gene expression in unexpected ways, as could the high levels of the protein produced from the ccg promoter. Therefore, we undertook a thorough examination of the electrophysiological phenotype of the his-tagged GFP strain.

The direct relationship between the current and voltage across a membrane can be simply stated by means of the equation:

$$V_M = IR \quad (\text{eqn 1.3})$$

Where V_M is the membrane voltage, I is the total membrane current (both passive and active) and R is the total resistance. Results showed the current-voltage relations of his-tagged mutants to be no different than those of the wild type strains. Due to the biological nature of the experiment, inevitably there is variability between trials, even within the same colony. However, mean values indicate (for an assumed identical resistance of both hypha and micropipette between trials) that there is no change in the net ionic current flux in the his-tagged GFP colonies. Although previous studies have shown the resting potential of the *Neurospora* membrane to be close to -175 mV (Gradmann *et al.* 1977), our results indicated an average resting potential of -130 mV. As well, documented values of cyanide-induced depolarization in *Neurospora* generally range between 40 to 70 mV. Our data showed a greater depolarization affect, averaging around 80 mV. An investigation of the ionic concentrations, pH and composition of the buffering solutions used in this experiment, compared to those used by Gradmann *et al.* (1977), did not reveal any noteworthy differences (with the exception of no $MgCl_2$, the ion concentrations and pH were the same). Another possibility for the discrepancy lies in the nature of the experimental preparations. Gradmann *et al.* (1977) skewered smaller branching hyphae located near the site of impalement. This resulted in cell death and sealing of septa connecting the hyphal units. Our experiments did not involve 'skewering', and we checked to show that the colonies continued normal growth. This may account for the more depolarized potentials we observed (due to uptake of nutrients to maintain sustained growth) and the increased level of cyanide inhibition (indicative of higher proton pump activity).

Since the primary source of active transport in fungi is the H^+ -ATPase, it was suggested that a diminished intracellular ATP supply due to extra protein production within the cell could cause a decrease in active current component. Therefore, although there was no difference in the current voltage relations between mutant and wild type colonies, we needed to separate out the passive ion concentrations from the activity of the pump. The use of cyanide in determining the relative

components of active and passive transport in the membrane of *Neurospora crassa* has been well documented in the literature (Gradmann *et al.* 1977). Because cyanide causes the potential to depolarize to the level of the Goldman-Hodgkin-Katz potential, contributions to membrane potential from both passive and active currents could be separated for further analysis (Fig. 4). Here, we have assumed that cyanide has no other major effects on the electrophysiology of the cell. The results revealed that there was no statistically significant difference in either current source between the two strains.

The conductance (g_m) is a measure of the overall electrogenic flux across the membrane (Hamam and Lew, 2012). In other words, it is the ability of a material to conduct electrical charge. From a physical point of view, the conductance can be calculated from the slope of the current voltage relation (Fig. 3). Earlier research showed that cyanide inhibition generally causes about 5% to 10% decrease in conductance across the membrane (Spanswick, 1981). Our data supports this trend: the average conductance is slightly less after cyanide treatment. The appearance of a slightly greater decrease in conductance for wild type cultures (Fig. 5) was statistically insignificant.

Although the use of green fluorescent protein is widespread throughout molecular biology, there appears to be little literature discussing its effects on the cell or on the particular protein to which it is fused. Here, we fill a gap in our scientific knowledge, revealing that high level expression of a GFP tag targeted specifically to the nuclei is without effect on the ‘physiological poise’ of the fungus, as measured by its electrical properties.

CONCLUSION

Overall, there were no significant differences between the electrophysiological characteristics of his-tagged mutant colonies compared to wild type. Our research supports the efficacy and versatility of green fluorescent protein for use in the laboratory.

REFERENCES

- Deschaneau, A.T., Cleary, I.A., Nargang, F.E. (2005) Genetic evidence for a regulatory pathway controlling alternative oxidase production in *Neurospora crassa*. *Genetics* 169:123-135.
- Freitag, M., Patrick, H. C., Namboori, R.B., Selker, E.U., Read, N.D. (2004) GFP as a tool to analyze the organization, dynamics and function of nuclei and microtubules in *Neurospora crassa*. *Fungal Genetics and Biology* 41: 897-910.
- Gradmann, D. Hansen, U.P., Long W.S., Slayman, C.L. Warncke, J. (1977) Current-voltage relationships for the plasma membrane and its principal electrogenic pump in *Neurospora crassa*: I. steady state conditions. *Journal of Membrane Biology*. 39; 333-367.
- Hamam, A. and Lew, R. (2012) The electrical phenotypes of calcium transport mutants in a filamentous fungus, *Neurospora crassa*. *Eukaryotic Cell*. 11:694-702.
- Lew, R. (2007) Ionic currents and ionic fluxes in *Neurospora crassa* hyphae. *Journal of Experimental Botany* 58: 3475-3481.
- Nobel (2008) "The Nobel Prize in Chemistry 2008 – Presentation Speech". Nobelprize.org. 22 Apr 2013 http://www.nobelprize.org/nobel_prizes/chemistry/laureates/2008/presentation-speech.html
- Patterson, G. H., Knobel S.M., Sharif, W.D., Kain, S.R., Piston, D.W. (2007) Use of the green fluorescent protein and its mutants in quantitative fluorescence microscopy. *Biophysical Journal* 73: 2782-2790.
- Serrano, R. (1984) Plasma membrane ATPase of fungi and plants as a novel type of proton pump. *Current Topics in Cellular Regulation* 23: 87-126.
- Spanswick, R.M. (1981) Electrogenic ion pumps. *Ann. Rev. Plant Physiol.* 32: 267-289
- Tsien, R.Y. (1998) The green fluorescent protein. *Annual Review of Biochemistry* 67:509–544.
- Vogel HJ. 1956. A convenient growth medium for *Neurospora*. *Microb. Genet. Bull.* 13:42–46.

APPENDIX

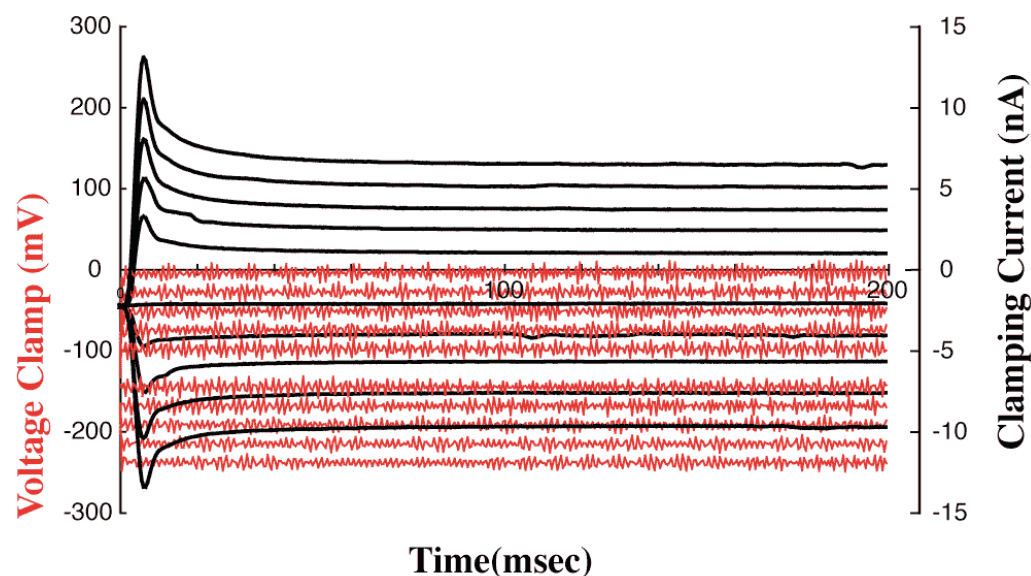
Prior to undertaking this experiment, we investigated the dependability of the voltage clamp to ensure the current-voltage relations were in steady state. Voltage clamping is a well-known method used for separating ionic and capacitive currents. This technique holds the membrane potential to a particular value, and measures the ionic current (called the clamping current) across the membrane.

For our purposes, the membrane of the cell can be modelled as a simple RC circuit, with a parallel resistance and capacitance. The current flowing through the membrane circuit is a combination of changes in the voltage and the ionic current:

$$I_m = I_i + C \frac{dV}{dt} \quad (\text{eqn A1.1})$$

Where C is the membrane capacity, I_i is the ionic current, and I_m is the membrane current. When the membrane potential is changed from one level to another, the rapidly changing voltage causes a short-lived spike, the capacitance current. However, once the voltage reaches a steady level, the capacitance current drops to zero. At this point, the ionic current may be measured. Therefore, it is essential that the voltage clamping be fast enough to ensure that the capacitance current reaches zero quickly. A representative voltage clamping experiment that show both voltage and the clamping current is shown in Figure 6.

Figure 6. Time dependent clamping currents. Both the clamped voltages (red) and clamping currents (black) are shown. Voltage was clamped at 10 values from 0 to -300 mV, and the corresponding current change was recorded in nA. The capacitance current can be seen as the initial current overshoot (capacitance spike), which lasted approximately 20 ms, after which the current reached steady state.



Generally, a voltage clamp measurement requires two electrodes (one for voltage measurement, the other for injecting current) and a feedback amplifier. The amplifier measures the membrane potential from the voltage-recording electrode and compares it to the chosen voltage-clamp value, called the ‘command voltage’. If there is a difference between these two signals, the feedback amplifier will amplify it, and inject the current necessary to match the measured voltage with the command voltage. It is important that the signal amplification is large, so that even slight variations between the command voltage and the membrane potential can be corrected. The ability of an amplifier to increase the strength of a signal is called the gain. In order for our amplifier to have a high gain, a very high feedback resistance is used. A circuit representation of the complete system (except the relatively complicated feedback amplifier) is shown in Figure 7.

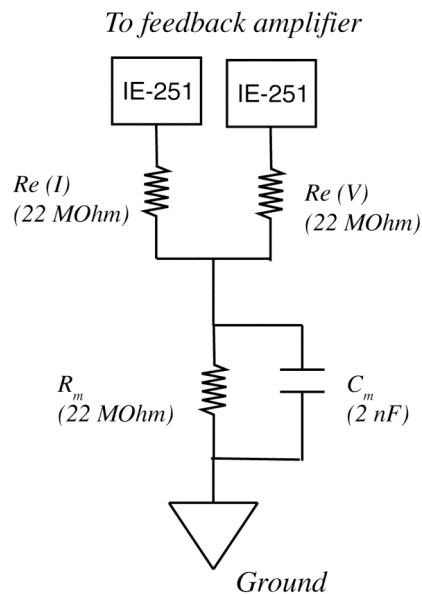


Figure 7. Model circuit for voltage clamp. (Left) Cell membrane is represented as an RC circuit connected to ground. Voltage-recording and current-injecting electrodes are shown as $R_e(V)$ and $R_e(I)$, respectively. Both electrodes are connected to the feedback amplifier and recording apparatus, marked as IE-251. (Bottom) Breadboard representation of the same circuit.

